NUMERICAL STUDY OF THE DISCRETE FREQUENCY NOISE GENERATION IN AN AXIAL FLOW FAN

K.M. Argüelles Díaz – J.M. Fernández Oro – C. Santolaria – P. Fernández Coto

Fluid Dynamics Group, Universiry of Oviedo.
Campus de Viesques, 33271 Gijón (Asturias), Spain.
arguelleskatia@uniovi.es

ABSTRACT

Aeroacoustics was firstly established in order to describe the noise produced by aircrafts. The optimization of propulsion systems in airplane engines lead to an important reduction of jet noise but other acoustic effects, like fan noise, were still an issue to deal with. The knowledge of the sources and the behaviour of noise will allow the development of procedures or actions to reduce sound levels. One possibility is the establishment of a methodology based on numerical simulations to characterize the aerodynamic noise.

Lighthill´s analogy was generalized later by Ffowcs Williams and Hawkings to be applied to turbomachines. Following the analogy, this paper presents a numerical methodology focused on the study of the generation and propagation of the discrete frequency noise in the far field in an axial flow fan. A hybrid approximation was employed to separate the aerodynamic and acoustic problem. Also, experimental results are carried out to validate the numerical methodology.

NOMENCLATURE

B	number of blades	R_0	blade radius (m)
c_0	sound velocity (m/s)	V	number of vanes
F(t)	lift force (N)	w	blade loading harmonics
F_{wV}	blade loading harmonics (N)	x	Bessel argument
$J_n(x)$	Bessel function	α	Pitch (rad)
m	BPF harmonics	θ	observer's angular position (rad)
M	source Mach number	φ	observer's angular position (rad)
n	Bessel order	φ_0	source's angular position (rad)
p'	sound pressure (Pa)	Ω	rotational frequency (rad/s)
R	observer's radial position (m)	Ω_{wV}	equivalent rotation speed (rad/s)

INTRODUCTION

Computational Aero-Acoustics (CAA) is a scientific discipline for the study of aerodynamically generated noise. The generation of aerodynamic noise may be characterized numerically by solving the compressible, unsteady Navier-Stokes set of equations. This method is known as the **direct approach** in which numerical results are obtained just from basic physical principles without needing experimental results or additional hypotheses. In this way both broadband and tonal noise may be resolved as well as mean flow patterns and unsteady pressure fields, all at once. This means a complete description of no linearity and all complex features associated with three-dimensional geometries. Recently, different works have studied CAA applications to particular cases. For instance, in the Second Computational Aero-Acoustics Workshop on Benchmark Problems (Tam, 1997) a model problem was related to turbomachinery noise, using a bidimensional gust response model. Four different solutions were discussed, with also significance differences between them. Basically, these discrepancies are due to poor spatial

discretizations and unsteady boundary conditions instabilities. A wide range of computational time is also typical, going from few minutes, if the solution is obtained in the frequency domain, to several hours, if the resolution strategy is based on the temporal one. The fan noise predictions require three-dimensional considerations, including blade rows from hub to tip (both fixed and moving ones), and accurate wake transport predictions. Therefore, in order to maintain a good precision in the calculations, the direct approach needs extremely high computational capacities which are not available today, so alternate methodologies are needed. Anyway, some CAA algorithms have been considerably enhanced, especially those related to parallel computing and CPU time economization (Tam, 1997, Lockard & Morris). Other algorithms have been also developed to reduce CPU times, achieving quite good performance, like the approximation known as Green's Function Discretization (GFD) (Caruthers, 1995). This strategy, recommended for three-dimensional CAA applications, reduces the number of grid points per acoustic wavelength, adjusting it to the Nyquist criterion.

Taking into account the great disparities between spatial and temporal scales, respectively, associated with both flow and acoustic fields, a reasonable option instead of the direct approach is decoupling the computational issue in two problems: a first one designed to resolve the flow field, and second one which will work on the sound field characterization. This methodology, known as **hybrid approach**, has a perfect example in the aero-acoustics analogy, because of the domain decomposition in other two sub-domains, one for the source zone and the other for the propagation. Aero-acoustic analogy theory transforms the Navier-Stokes equations in an inhomogeneous wave equation with source terms related to the acoustic sources. Consequently, the flow field is obtained in an independent fashion from the acoustic field, using traditional CFD methods in order to characterize acoustic sources. Under the free-field conditions, that is, when a reverse influence of the acoustics on the flow is not possible, then sound propagation onto far field may be evaluated through numerical resolution of an integral formulation.

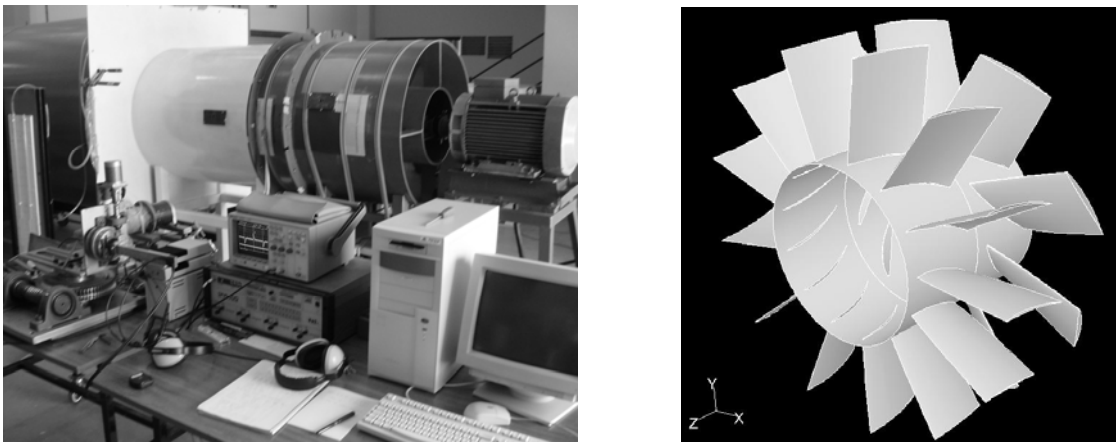

Figure 1. Axial turbomachine facility. Detail of the fan stage.

The main scope of this work is based on the numerical characterization of the noise generation of an axial flow fan, with the help of aero-acoustic analogy. For this purpose, an industrial fan facility, previously developed for farming purposes, is used. The fan is composed of one single stage with an upstream stator of 13 stationary vanes followed by a 9 blade rotor. The design rotational speed is 2400 rpm, the nominal flow rate is about 18 m^3/s, and tip and hub diameters are, respectively, 820 and 380 mm. Figure 1 shows an image of the experimental facility and a sketch of the fan stage. To obtain the acoustic sources in the numerical procedure, a CFD commercial software (Fluent) has been employed. The numerical characterization of the propagation zone is resolved in the frequency domain, using the integral solution of the Ffowcs Williams and Hawkings

(FFWH) equation. The calculation has been realized in a C++ source, with the acoustic sources, obtained by an unsteady CFD solution, as input data.

Fan tonal noise is generated by the interactions of a rotor, isolated or embedded in a stage, and the flow disturbances. Although three-dimensional configurations are beginning to be taken into account, most of the investigations had been carried out for bidimensional configurations. A typical approach, used to predict interaction tonal noise, is based on a modal analysis of the Tyler and Sofrin theory (Tyler, 1962). This methodology introduces blade wakes as vortical gusts, addressed through empirical correlations obtained from scale models, or even through numerical simulations results. This approach employs a "source" model for the determination of the blades unsteady pressure fields. Generally, the blades are considered as a cascade of bidimensional flat planes. Diverse models and codes have been developed (Ventres, 1982), (Eversman, 1995) and (Meyer, 1996), but all of them need a more accurate aerodynamic input data, improving their grid resolutions for a better description of three-dimensional features of the flow like secondary flows. Also, a reduction in CPU times is desirable.

THEORETICAL FORMULATION

Lighthill aero-acoustic analogy (Lighthill, 1952) is used to study the problem of aerodynamically generated noise, through decoupling the domain of interest in two zones: the source zone and the propagation one. However, there are some restrictions that limit the application range of this theory, so, sometimes, is necessary to enhance the analogy by taking into account collateral effects like compressible fluid mechanics, non-uniform flows, or solid walls in the source zone. The usual version of the Lighthill analogy is the FFWH theory, because of the inclusion of wall effects and all type of motions (Ffowcs Williams and Hawkings, 1969).

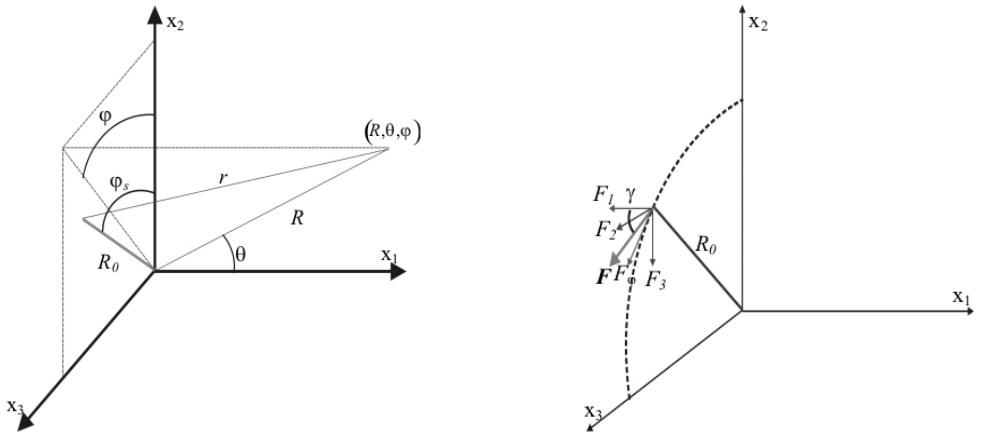

Figure 2. Frame of reference for the radiated noise of a rotating dipole.

The key point of FFWH was based on the definition of an equivalent environment where real bodies are replaced by mathematical surfaces. Also, it is assumed that the inner volume of those surfaces contains quiet surrounding flow (Farassat, 1974). The most usual expression of FFWH equation is obtained when these mathematical control surfaces are matched with the solid surfaces (therefore, the no slip condition establishes that the fluid velocity in contact with the surface is exactly the same as the surface velocity), and also when the next hypotheses are satisfied: the flow Reynolds number is high (inertial terms are predominant over the viscous ones), flow Mach number is low (the flow is practically incompressible) and the flow is isentropic. In this way, the source terms of the FFWH correspond to quadrupolar (volumetric source), monopolar and dipolar (superficial sources) radiation sources, according to its mathematical structure.

The quadrupolar radiation term is not very important – in comparison to the monopole and the dipole – when generated sound sources in motion are traveling at subsonic velocities, so their

effects can be negleted (Brentner, 2000). The monopolar source term is completely defined by surface kinematics and represents what is called as **thickness noise**. In case of low Mach number flows and with thin blades, thickness noise has no relevance and can be obviated. In other hand, when turbomachinery generated noise is studied – i.e. when fluctuating forces come from rotating blades – the dipolar source term is reduced just to the blade loads (lift and drag), and represents the **loading noise**. This kind of noise is precisely the most efficient from an acoustic point of view and is responsible of the noise propagation in the far field (Roger, 1996).

This problem can be dealt with using the FFWH analogy (Ffowcs Williams, 1992). Nevertheless, it is necessary to solve the equation in retarded time when you are using this formulation directly in the temporal domain. Retarded time means that for every observer's time, it is necessary to establish the appropriate emission time of the source and its location. Obviously, this process requires high computational effort. Anyway, when the study of turbomachinery discrete frequency noise in a subsonic rotational regime is attempted, the object is to obtain its acoustic spectrum, so the accurate procedure is to solve the problem in the frequency domain, avoiding the need to resolve the equation in retarded time.

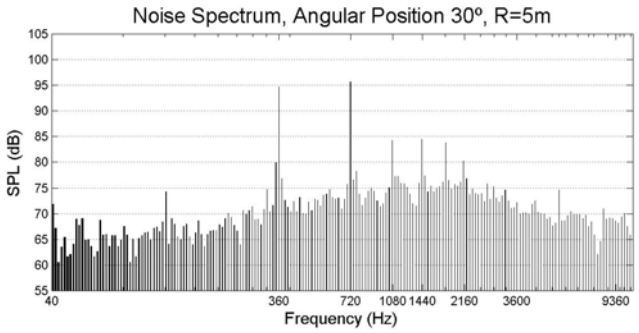

Figure 3. Typical rotor noise spectrum (log scale).

The typical noise spectrum of a rotor (Figure 3) always contains a broadband part and one of discrete frequency, at the **blade passing frequency** (BPF) (number of blades times the rotational frequency) and its harmonics. The Sound Pressure Level (SPL) generated at blade passing frequency, is called **tone**. A portion of the blade at radius R_0, rotating at constant angular frequency Ω, and under low Mach number conditions, behaves as an acoustic dipole of intensity **F**(t), where **F**(t) is the blade loading (supposed a low and constant pitch degree γ respect to the rotation axis). It is assumed that **F**(t) has only tangential and axial components since this configuration fits typical axial flow turbomachines (Figure 2). Besides, large number of fan designs include an stator of V vanes upstream the rotor with B blades, which leads to a spatial harmonic variation of the incident flow at angular period $2\pi/(V\Omega)$. Under this configuration, the rotor is still the principal noise generating source and the acoustic pressure fluctuations are still produced at blade passing frequency and harmonics, which can be computed in the far field according to (Roger, 1996):

$$p'(\vec{x},\omega)=\sum_{m=-\infty}^{\infty}\sum_{w=-\infty}^{\infty}\frac{imB^2\Omega e^{imB\Omega R/c_0}}{4\pi c_0 R}e^{i(mB-wV)(\varphi-\pi/2-\varphi_0)}\left[\cos\gamma\cos\theta-\frac{mB-wV}{mB}\frac{c_0}{R_0\Omega}\sin\gamma\right]J_{mB-wV}(mBM\sin\theta)F_{wV} \qquad (1)$$

where M is the Mach number source, and $J_n(x)$ is the Bessel function of type n. The complex coefficients F_{wV}, so called blade loading harmonics, are obtained in the same way as Fourier series coefficients of function F(t). When the rotor blade can not be considered as compact, the expression (1) is applied to every compact sub-segments that divides the blade.

Expression (1) points out that the periodic blade load working over the rotor blades generates sound at passing blade frequency ($mB\Omega$) and its harmonics. Consequently, the acoustic pressure

fluctuations, noticed by an observer placed in the far field, are composed by an infinitive sum of the characteristic radiation modes of the free-field. The magnitude of every radiation mode is proportional to a blade load harmonic weighted by a Bessel function that is responsible for a modulation in the source frequency. Also, every radiation mode spins at an angular velocity that is given by the expression $\Omega_{wV} = (mB\Omega)/(mB - wV)$. When $wV \neq mB$, the appropriate radiation mode is called **spinning radiation mode**, and does not take part in the propagation of noise to the far field along the fan axis. When $wV = mB$, the radiation mode is called **symmetric mode**, responsible for the radiation along the fan axis. In particular, radiation mode $w = 0$, is associated to the radiated noise by the stationary part of the blade loads over the rotor blades (Gutin noise).

NUMERICAL METHODOLOGY

The acoustic sources of the radiated noise into the far field will be bipolar order sources distributed over the blade surfaces. This assert is due to the fact that just the blade load term is going to be considered in our study, avoiding other terms for the simulation in the frequency domain. Because of the equidistant circumferential distribution of the blades, it is possible to determine the dipolar acoustic sources by focussing on just one blade (this implies that all the blades are identical).The influence of the other blades is included through an interference function of the rotor. This way, the sound pressure spectrum in the far field that fits to the stator-rotor interaction, will be expressed by equation (1) when is applied to every compact sub-segments of every blade division. The source zone has been characterized through an unsteady CFD modelling, using a sliding mesh technique for the rotor. The mesh reaches up to 1.8 million cells, with intensive refinement around the blade surfaces. A grid distribution of [80x60x25] was adopted for every blade channel (13+9 for the complete machine).

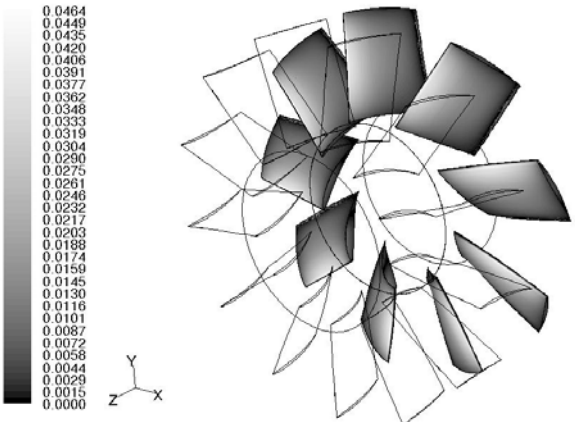

Figure 4. Non dimensional instantaneous blade load over rotor blades.

Load harmonics are calculated with the Fourier transform of the blade load temporal series. Figure 4 shows the blade load distributions over the rotor blades at one instant. If the blade would be compact, then only the total blade load temporal series will be obtained. But if the blade is not compact, then it is necessary to divide it into compact sub-segments and obtain separately the load harmonics related to the temporal series of the blade load over those sub-segments. The total effect of these sub-segments is achieved through a double integration over the blade surfaces in both span and blade chord directions.

In order to simplify the coupling between the Fluent numerical results and the numerical resolution of equation (1), we have matched the compact sub-segments with the spatial discretization of the grid over the blade surfaces. For every cell, Fluent provides a temporal series of the local blade load that are used as input data for the C++ program. Next, the post-processing program computes every blade load harmonic using the FFT algorithm. For ensuring the accurate

response of the FFT algorithm, the numerical simulation in Fluent is fit to such a time step size that 512 intermediate positions per rotor turn are guarantied.

The geometrical parameters of every discrete cell over the blade surfaces are also provided by the Fluent simulation (the radius and the angular coordinate are supposed to be concentrated in the rotor plane). The observer's position, in which the sound level of the radiated noise by the fan is going to be calculated, is introduced through spherical coordinates that must be kept fixed for every noise calculation. It means that the post-processing of Fluent data must be repeated for all the desired observer's locations.

The directional characteristics of the noise spectrum radiated to the far field are provided by Bessel functions that are included in the equation (1). Consequently, in the post-processing code an algorithm for the Bessel function treatment has been implemented.

In the expression (1) there is an infinite sum of index w over all the blade load harmonics, and another infinite sum of index m over the blade passing frequency harmonics. For a fixed m, it is possible to get the sound pressure of the blade passing frequency $mB\Omega$, allowing to realize an analysis of every harmonic contribution onto the total sound spectrum. Due to the behavior of the Bessel functions and its attenuation characteristics (Figure 5), for a particular blade passing frequency only few blade load harmonics may contribute to the radiated noise to the far field, so the sum over the index w converges quickly. The total sound spectrum will be the sum of the contributions at every blade passing frequency, that is, of the results obtained for every value of index m (m values must be added until sum convergence is achieved). The signal in the temporal domain can be restored using the inverse Fourier transform of the noise spectrum.

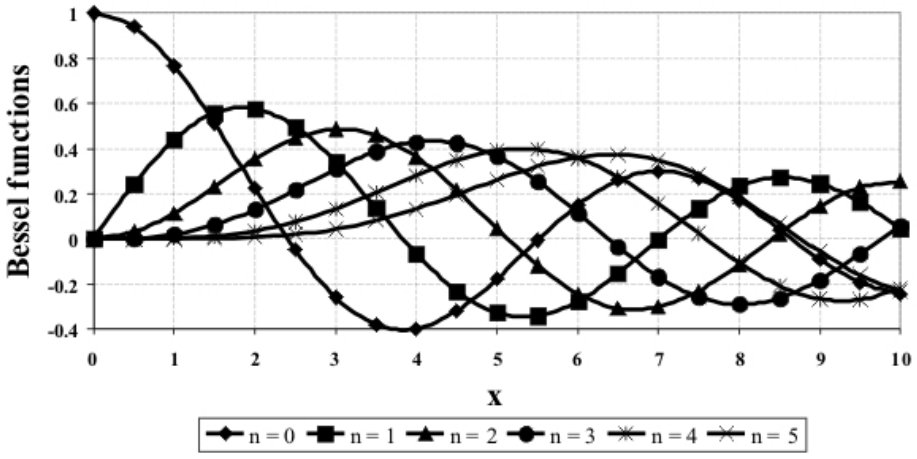

Figure 5. Attenuation of increasing type Bessel functions.

RESULTS

Following the methodology described in the previous part of the paper, a numerical simulation of the aero-acoustic behavior of the axial flow fan was generated, taking the source zone data, obtained via CFD simulation, as the first step. The numerical simulations have been executed for three circular sectors, placed at the horizontal zx plane, at the axis height. The radial distances adopted with respect to the fan rotor are at five, seven and nine meters. These planes will be denoted R5, R7 and R9 respectively. The observer position is established over every of these circular sectors at regular angular intervals of five degrees. This means that 0º degrees indicates the point located right upstream of the stator, and the angle of 180º indicates the point placed just behind the rotor (Figure 9). The fan is supposed to be operating at nominal conditions, that is, at a nominal speed of 2400 rpm (40 Hz) and therefore with a blade passing frequency of 360 Hz. Finally, numerical results will be compared with experimental measurements acquired at analogous points. Experimental uncertainty is placed on ± 2 dB, for a 95% confidence interval.

Turbulence models comparison

Past investigations by CAA seem to demonstrate that Large Eddy Simulation (LES) turbulence modeling captures aero-acoustics scales with more accuracy than the traditional Reynolds Stress Model (RSM). The prediction on fan noise needs a good resolution of the flow vortical structures in a wide range of spatial scales. Traditional turbulent closure strategies for RANS modelling are not so accurate to undertake this kind of problems. So it is necessary the use of more complex turbulence models, in spite of higher computational efforts, like the LES scheme, that is able to resolve directly the bigger vortexes of the flow pattern, which are responsible for the noise generation in turbomachinery (Mendoza and Allen, 2002). In the other way, the small scales use to be weaker, with less energetic contain and a characteristic isotropic, universal character, so they can be modelled in a generic way. Taking into account that noise generation is a clearly unsteady process, the LES scheme seems to be the most powerful tool in the obtaining of fan noise nowadays. To validate the previous assertion, we have realized acoustics simulations using input data computed with LES and RSM turbulence models. Figure 6 shows results of both numerical simulations at R5 plane for the SPL of the blade passing frequency and for the total SPL. Also they are compared with experimental results. The total numeric SPL is obtained through an expression that includes the SPL of the BPF and its harmonics:

$$SPL_{\text{total}} = 10\log\left(10^{SPL_{\text{BPF}}/10} + 10^{SPL_{2\text{BPF}}/10} + \ldots + 10^{SPL_{n\text{BPF}}/10}\right) \quad (2)$$

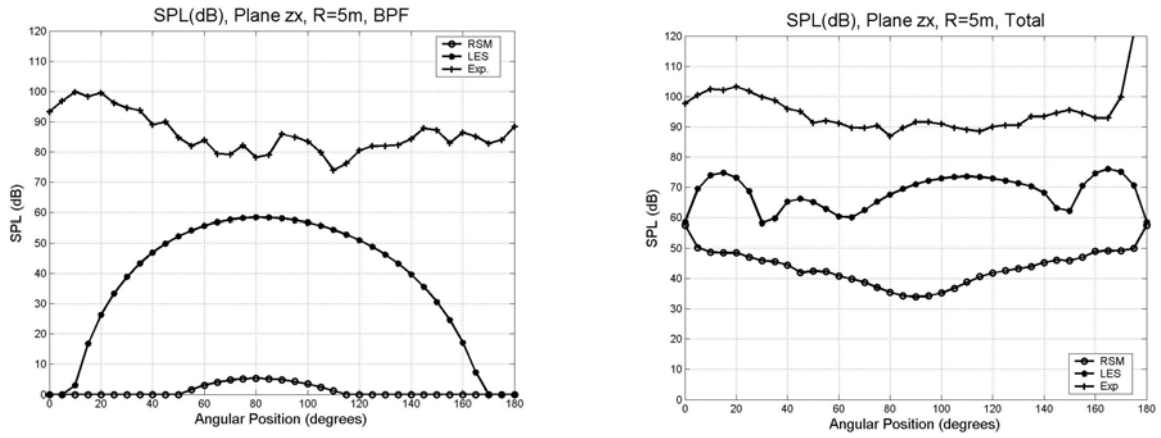

Figure 6. Comparison between turbulence models.

As it can be seen in Figure 6, LES modelization captures in a better fashion the characteristics of the acoustic field radiated into the far field, not only qualitatively but also in the SPL range. Meanwhile, RSM model is under-estimating the SPL by far. At first glance, the differences in the SPL predicted by the LES modelization and the one obtained experimentally is owing to the existence of additional real sources that have not been taken into account in the numerical simulations, like broadband noise, turbomachine driven motor noise, trailing edge noise, etc. Also, operational reasons force the fan to be ducted with a casing; this feature produces a displacement of the aero-acoustics behavior of the turbomachine from the expected theoretical descriptions of free-field conditions at the angular interval between 40º and 140º, approximately. In the rest of angular positions, LES modeling captures with quite good agreement the sound field of the axial flow fan. Differences between numerical and experimental results at BPF are due to the existence of other tone acoustic sources not considered in the modelling, like thickness noise. From now on, for the rest of the simulations, just the LES scheme was employed for the comparison with experimental results.

SPL variation according to source distance

Figure 7 shows the variation of the SPL with the radial distance to the fan axis. The graphic presents numerical and experimental results of SPL at blade passing frequency and total SPL, for the already mentioned R5, R7 and R9 planes. Both numerical and experimentally SPL attenuates as long as the observation point goes far away from the acoustic source, as it was expected to be from the spherical waves features. Notice how the duct of the fan is modifying the experimental results. The attenuation, according to the numerical results is about 2 dB, meanwhile experimentally, for the zones where the fan casing is not affecting the acoustic behavior at free-field, the attenuation is slightly more pronounced, about 5 dB.

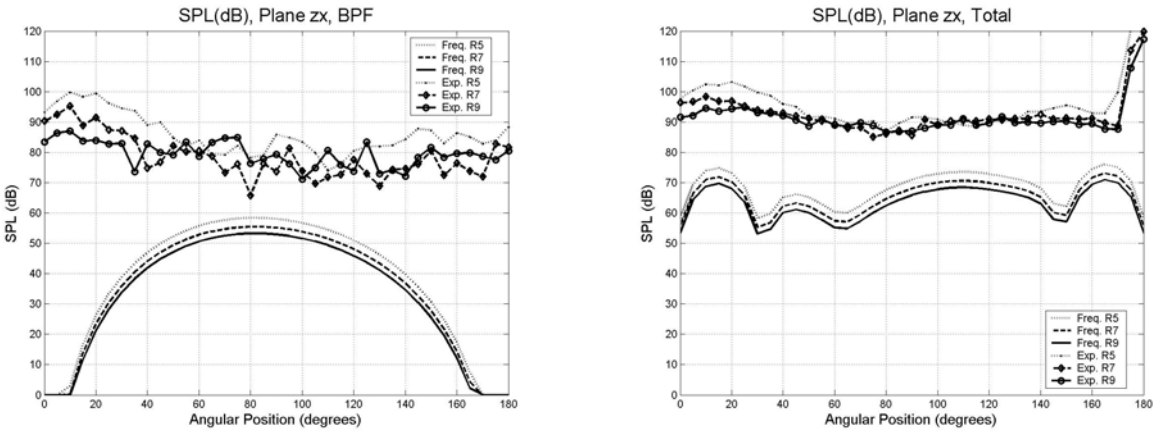

Figure 7. SPL variations with radial distance.

Directional patterns

Figure 8 presents directional patterns, both numerical and experimental, of the SPL at the blade passing frequency for R5 plane.

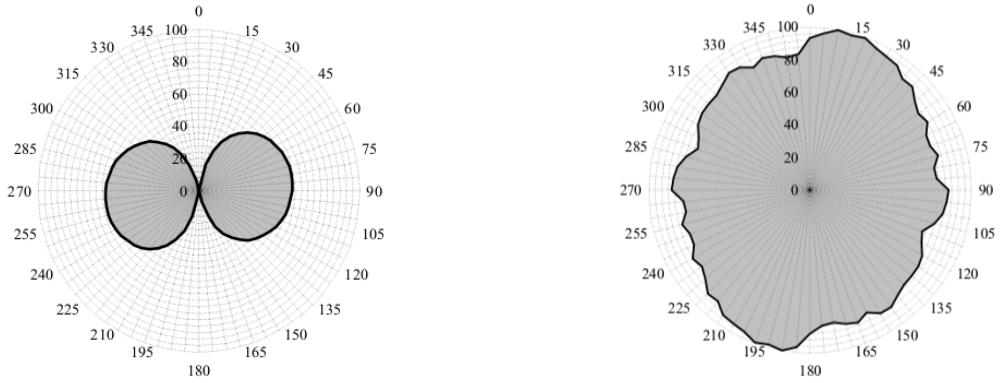

Numerical, BPF, R=5m Experimental, BPF, R=5m

Figure 8. Sound field directivity of the flow fan.

Because of the 13 stator vanes placed upstream the 9 rotor blades, the symmetric mode of radiation, responsible of the radiation on the fan axis, is never generated for this turbomachine. So far, theoretically, because of the Bessel functions behavior of equations (1) (Figure 5), radiation minimum values must be located along the axis. On the other hand, the maximum values will be at 90º from the axis. Besides, if it is kept in mind that the only source term has dipolar order, the directional character of the radiating noise to the far field must be clearly identified with a dipole one. The dipole is clearly present in the plot of the numerical results of the SPL at blade passing frequency, with minimum values along the fan axis. Experimentally, because of the presence of

additional noise sources, the dipole character is much more diffuse. Anyway, at blade passing frequency, it can be guessed the presence of minimum values of radiation on the axis and maximum values at normal direction.

Figure 9 shows directional patterns of total SPL, and its attenuation along the distance for the R5, R7 and R9 planes. In this case, the experimental acoustic behavior is totally masked by the presence of the turbulence associated to the fan jet, so the noise at discrete frequency is dominated by the broadband noise at low frequencies.

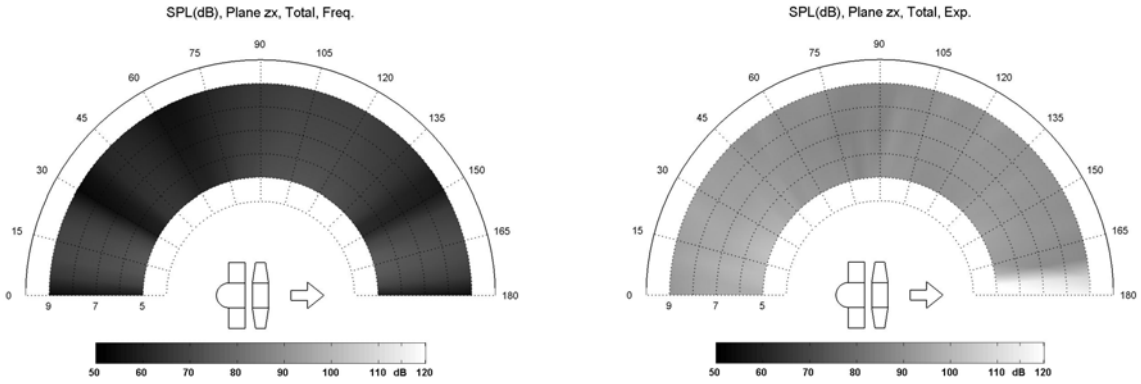

Figure 9. Directivity at plane zx for the axial fan.

This statement is validated with the spectra of Figure 10, representing an angular position of 90º with respect to the fan axis and for a point situated downstream the rotor. In the second of these angular positions, the sound spectrum is clearly dominated by the broadband noise of the jet; meanwhile at 90º of the fan axis, blade passing frequency tones and its harmonics can be noticed.

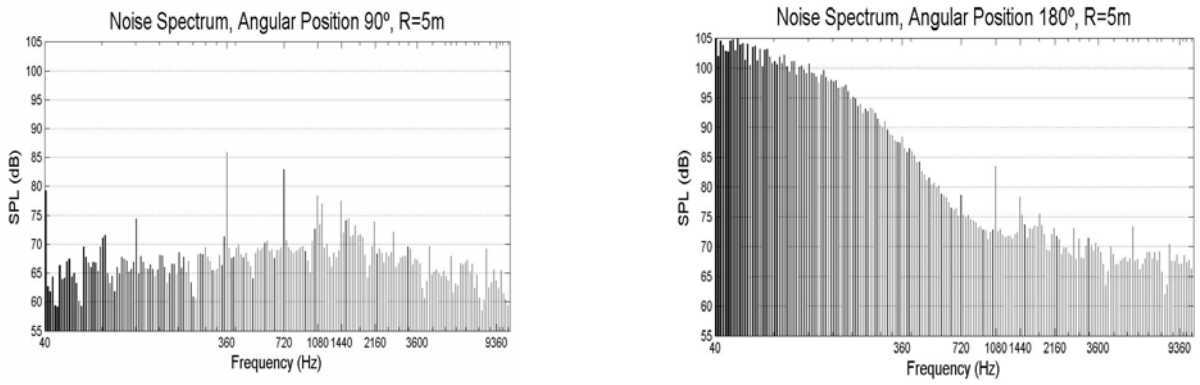

Figure 10. Experimental noise spectrum at 90º and 180º angular positions.

CONCLUSIONS

Aero-acoustic behavior in the far field for a stator-rotor configuration in an axial flow fan has been studied theoretical and numerically, based upon the aero-acoustic analogy solved in the frequency domain. The obtained results have been compared to experimental measurements.

The source zone has been characterized with a numerical CFD simulation of the flow structure inside the fan, that is, resolving the set of incompressible Navier-Stokes equations. LES turbulence model has demonstrated better features compared to the RSM model for the noise predictions in the far field, that had been carried out through the implementation of a post-processing program based on the integral solution of the FFWH equation in the frequency domain. Future work will compare numerical results obtained in the frequency domain with similar calculations realized in the temporal domain.

In general, a reproduction of the real aero-acoustic behavior of the fan has been achieved with the numerical simulation. The numerical model is valid in all zones, except for the jet affected region in which broadband noise is dominant. For the rest zones, discrepancies can be attributed to the presence of other noise generation mechanisms: thickness noise, tip vortex, broadband noise, etc., that will have to be included in the numerical model for next works.

Definitively, a useful tool for noise prediction is available to characterize the acoustic behavior of the turbomachine in the design process, in order to adopt accurate actions to reduce the sound emission levels of the machine.

ACKNOWLEDGEMENTS

This work was supported by the Research Project "Modeling of deterministics stresses in axial turbomachinery", ref. DPI2003-09712, CICYT.

REFERENCES

Brentner, K.S., (2000). *Recent advances in rotor noise predictions*. AIAA-2000-0345.

Caruthers, J.E., French, J.C. and Raviprakash, G.K., (1995). *Recent Developments Concerning a New Discretization Method for the Helmholtz Equation*. CEAS/AIAA-95-117.

Farassat, F., (1974). *The acoustics far-field of rigid bodies in arbitrary motion*. J. Sound and Vibration. Vol. 32.

Ffowcs Williams, J.E. and Hawkings, D.L., (1969). *Sound generation by turbulence and surfaces in arbitrary motion*. Phil. Trans. Roy. Soc. A 264.

Ffowcs Williams, J.E., (1992)**.** *Modern methods in analytical acoustics*. Springer Verlag.

Lighthill, M.J., (1952). *On sound generated aerodynamically I. General Theory*. Proc. Roy. Soc. A 211.

Lighthill, M.J., (1954). *On sound generated aerodynamically II. Turbulence as a source of sound*. Proc. Roy. Soc. A 211.

Mendoça, F. and Allen, R., (2002). *Towards understanding LES and DES for industrial aeroacoustics predictions*. International workshop on LES for acoustics, Germany.

Roger, M., (1996). *Applied aeroacoustics: prediction methods*. Von Karman Institute for Fluid Dynamics, Lecture Series 1996-04.

Tam, C.K.W. and Hardin, J.C., (1997). *Second Computational Aeroacoustics (CAA) Workshop on Benchmark Problems*. NASA CP-3352.

Tayler, J.M. and Sofrin, T.G., (1962). *Axial Flow Compressor Noise Studies*. SAE Trans., Vol. 70, pp. 309-332.

Ventres, C.S., Theobald, M.A. and Mark, W.D., 1982. *Turbofan Noise Generation*. NASA CR-167952, Vols. 1 and 2.

Meyer, H.D. and Envia, E., 1996. *Aeroacoustics Analysis of Turbofan Noise Generation*. NASA CR-4715.

Eversman, W. and Danda, R.L., 1995. *Ducted Fan Acoustic Radiation*. CEAS/AIAA-95-155.